2013

Reactive self-heating model of aluminum spherical nanoparticles

Karen S. Martirosyan
The University of Texas Rio Grande Valley

Maxim Zyskin
Rutgers University - New Brunswick/Piscataway

Reactive self-heating model of aluminum spherical nanoparticles

Karen S Martirosyan[1,a)] and M. Zyskin[2]
[1]*Department of Physics and Astronomy, University of Texas, Brownsville, 80 Fort Brown, Brownsville, Texas 78520, USA*
[2]*Rutgers University, 126 Frelinghuysen Road, Piscataway, New Jersey 08854-8019, USA*

(Received 30 September 2012; accepted 21 January 2013; published online 6 February 2013)

Aluminum-oxygen reaction is important in highly energetic and high pressure generating systems. Recent experiments with nanostructured thermites suggest that oxidation of aluminum nanoparticles occurs in a few microseconds. Such rapid reaction cannot be explained by a conventional diffusion-based mechanism. We present a rapid oxidation model of a spherical aluminum nanoparticle, using Cabrera-Mott moving boundary mechanism, and taking self-heating into account. In our model, electric potential solves the nonlinear Poisson equation. In contrast with the Coulomb potential, a "double-layer" type solution for the potential and self-heating leads to enhanced oxidation rates. At maximal reaction temperature of 2000 °C, our model predicts overall oxidation time scale in microseconds range, in agreement with the experimental evidence.
 [http://dx.doi.org/10.1063/1.4790823]

Many previous studies have been directed to understand the mechanism and kinetics of aluminum particle oxidation.[1–9] The oxidation of aluminum exhibits high enthalpy and has been extensively used for propulsion, pyrotechnics, and explosion reactions.[10,11] Nanoenergetic materials (NM) based on aluminum thermites may store two times more energy per volume than conventional monomolecular energetic materials.[12] The size reduction of reactant powders such as aluminum from micro- to nano-size increases the reaction front propagation velocity in some systems by two to three orders of magnitude.[12,13] Among numerous thermodynamically feasible metastable intermolecular composites mixtures, the most widely investigated are Al/Fe_2O_3, Al/MoO_3, Al/WO_3, Al/CuO, Al/Bi_2O_3, and Al/I_2O_5 nano systems.[12–20] The main distinguishing features of these reactive systems are their significant enthalpy release and tunable rate of energy discharge, which gives rise to a wide range of combustion rates, energy release, and ignition sensitivity.

There are several advantages of using Al/Bi_2O_3 and Al/I_2O_5 nanocomposites: (i) reduced ignition and reaction times; (ii) superior heat transfer rates; (iii) tunability of novel energetic fuel/propellants with desirable physical properties; (iv) enhanced density impulse; (v) incorporating nanoenergetic materials into micro- and nano-mechanical systems.[12] Our recent experiments suggest that oxidation of nanoparticles of aluminum with Bi_2O_3 and I_2O_5 occurs in a few microseconds.[17–19] Rapid reaction in the nanostructured thermites cannot be explained by a conventional mechanism based on the diffusion of Al and O atoms in oxides.

In this report, we present a rapid oxidation model of spherical aluminum nanoparticles surrounded by oxygen, using Cabrera-Mott oxidation model[7–9] with a self-consistent potential, and taking self-heating into account. Using nonlinear self-consistent potential in Cabrera-Mott model, as opposed to the Coulomb potential, is more accurate, and yields higher oxidation rates. For nanosized particles, nonlinear model gives "double-layer" type solution for the potential, since potential changes rapidly near the metal-oxide interface. As a result, the electric field at the metal-oxide interface, determining the oxidation rate, is less sensitive to oxide thickness, and stays nearly constant at intermediate stages of oxidation (while for the Coulomb potential, electric field decreases and the oxidation rate quickly drops). This nonlinear effect for the potential, combined with self-heating, leads to rapid temperature increase, resulting in a dramatic (orders of magnitude) increase of oxidation rates for nano-sized particles. Our model can predict oxidation times in microseconds range, in a good agreement with the experimental data.[12]

To estimate the reaction times, we assume that aluminum sphere (radius 25 nm, with thin oxide layer of 3 nm) is surrounded by oxygen. The sphere is rapidly heated to ignition temperature T_0, sufficient to initiate oxidation reaction, further boosted by self-heating as a result of oxidation. We assume the spherical symmetry of the problem.

In the Cabrera-Mott model of metal oxidation,[1–4,7] aluminum ions are helped to escape aluminum boundary (overcoming the ionization potential W) by a self-consistent electric potential V. The electric field is induced in the oxide layer near the metal-oxide interface by imbalance of concentrations of positive aluminum ions $Ne^{-\frac{eV}{k_bT}}$ and excess electrons $Ne^{\frac{eV}{k_bT}}$. The pre-factor N is the concentration of charges far from the metal-oxidizer interface and is given by Eq. (2). Since concentrations of charges depend on the electric field itself, we arrive at a self-consistent version of the Poisson equation for V. In the spherically symmetric case, it is given by

$$\nabla^2 V \equiv \frac{1}{r^2}\frac{d}{dr}\left(r^2\frac{d}{dr}V\right) = 8\pi k_0 \mathbf{e} N \sinh\left(\frac{\mathbf{e}V}{k_bT}\right), \quad r_1 \le r \le r_2, \qquad (1)$$

$$V(r_1) = V_0,$$

$$V(r_2) = 0.$$

Here, r_1 is the metal particle radius, $(r_2 - r_1)$ is oxide layer thickness, k_0 is the electrostatic constant, $\mathbf{e}$ is the elementary

a)karen.martirosyan@utb.edu.

charge, $N = (n_e n_i)^{1/2}$, and n_i and n_e are given by $n_e = 2(2\pi m_e k_b T/h^2)^{3/2}\exp\left(-\frac{e\phi}{k_b T}\right)$, $n_i = N_i \exp\left(-\frac{eW_i}{k_b T}\right)$, where m_e is the mass of electron, k_b Boltzmann constant, h Plank constant, N_i is the concentration of sites available for hopping metal ions. Thus,

$$N = (n_e n_i)^{1/2} = N_0\left(\frac{T}{T_0}\right)^{\frac{3}{4}}\exp\left(-\frac{\mathbf{e}(\phi + W_i)}{2k_b T}\right),$$
$$N_0 = (2N_i)^{\frac{1}{2}}(2\pi m_e k_b T_0/h^2)^{3/4} \sim 1.5\,10^{27}\mathrm{m}^{-3},\ T_0 \sim 750\,\mathrm{K}. \quad (2)$$

The physical meaning of W_i is the difference of chemical potentials for metal ions in the metal and the oxide; ϕ is the potential difference for electrons in the conduction bands of aluminum metal and the oxide (a semi-conductor); and the value of V_0 is determined from the condition that metal ion concentration at the interface with the oxide equals n_i. In Cabrera-Mott model, those ionization potentials may be considered as model parameters.[7–9]

Oxidation of metal occurs via tunneling of aluminum ions into the oxide layer, overcoming ionization potential of maximum height $W > W_i$, and assisted by the self-consistent electric potential. Electric field provides potential energy decrease for ion hopping from the bottom to the top of ionization potential, at a distance of $\alpha_0 \sim 0.4\,\mathrm{nm}$. This leads to an equation for the metal-oxide interface radius r_1: the normal velocity of the metal boundary u_n is determined by the electric field $(-\nabla V)$ at the boundary, appearing in a Gibbs factor

$$u_n \equiv \frac{dr_1}{dt} = -\Omega_1 \nu n_2 \exp\left(\frac{-eW}{kT}\right)\exp\left(\frac{qe\alpha_0|V'(r_1)|}{k_b T}\right); \quad (3)$$
$$r_1(0) = r_{10}.$$

Here, r_{10} is the initial metal sphere radius, which we assume to be $22\,\mathrm{nm}$, $\Omega_1 \approx 0.0166\,\mathrm{nm}^3$ is the volume of oxide per aluminum ion, $n_2 \sim 10\,\mathrm{nm}^{-2}$ is the number of metal ions per unit surface area, $\nu \sim 10^{12}\,\mathrm{s}^{-1}$ is the frequency of tunneling attempts, $q = 3$ is aluminum valency.

In the Cabrera-Mott model, it is assumed that escaped metal ions migrate to the outer boundary of the oxide where they react with the oxygen, while local Gibbs distribution of excess densities of electrons and metal ions inside the oxide is essentially unaffected. Due to the spherical symmetry, the radius of the oxide-oxidizer interface r_2 changes uniformly, and can be found from conservation of the number of metal ions, taking into account difference in volumes per metal ion in the metal and the oxide, $(r_2^3 - r_{20}^3) = -\kappa(r_1^3 - r_{10}^3)$. Thus,

$$r_2 \equiv r_2(r_1) = \left(r_{20}^3 + \kappa(r_{10}^3 - r_1^3)\right)^{\frac{1}{3}}, \quad \kappa \approx 0.386. \quad (4)$$

Here, $r_{20} = r_{10} + \delta$, where $\delta \sim 3\,\mathrm{nm}$ is the initial oxide layer thickness.

For small metal particles, it is important to take *self-heating* into account, due to heat released by exothermic aluminum oxidation, resulting in temperature increase of the remaining metal and oxide layer. For nano-sized particles, temperature can be assumed to be uniform. Thus, temperature can be computed based on reaction heat release and specific heats of reagents. Assuming constant specific heats,

$$T \equiv T(r_1) = T_0 + \frac{\sigma H_{\mathrm{Al}}\rho_{\mathrm{Al}}(r_{10}^3 - r_1^3)}{c_{\mathrm{Al}}\rho_{\mathrm{Al}} r_1^3 + c_{\mathrm{Al_2O_3}}\rho_{\mathrm{Al_2O_3}}(r_2^3 - r_1^3)}. \quad (5)$$

Here, $\rho_{\mathrm{Al}}, \rho_{\mathrm{Al_2O_3}}$ are densities of the aluminum and oxide, $c_{\mathrm{Al}}, c_{\mathrm{Al_2O_3}}$ are specifics heats per unit mass, H_{Al} is the oxidation reaction enthalpy per unit mass of aluminum, and σ is the proportion of released heat which is used up for self-heating. We take reaction initiation temperature $T_0 = 750\,\mathrm{K}$. Since r_2 can be found from r_1 using Eq. (4), the temperature T in Eq. (5) is determined by r_1. Due to high enthalpy release in aluminum oxidation (~24 kJ per gram of aluminum), adiabatic assumption $\sigma = 1$ yields unrealistically high maximum temperature, even when melting and vaporization heats are taken into account. We assume that $\sigma = 0.11$ of the heat released contributes to self heating, while the rest is lost due to radiation, heat conduction, and convection. For such value of σ, the maximum reaction temperature, corresponding to $r_1 = 0, r_2 = r_2(0)$ in Eqs. (4) and (5), will be $T_M \sim 2000\,^\circ\mathrm{C}$, which agrees with the experiments.[12]

We use experimentally determined maximum temperature to control the effect of the heat transfer process on oxidation rates. Detailed modeling of the heat transfer is outside the scope of this letter. However, we note that an assumption of fairly large heat loss is sensible. For a nanoscale particle, the convection loss mechanism is important. Indeed, in the steady state limit, heat loss of a small sphere due to convection can be modeled by the Newton's law of cooling, with the heat transfer coefficient $\eta, [\mathrm{W\,m^{-2}\,K^{-1}}]$, given by $\eta = \frac{k}{r}$,[21] where $k, [\mathrm{W\,m^{-1}\,K^{-1}}]$, is air's thermal conductivity, and r is Al sphere radius (this limit is applicable for small Grashof numbers, which is the case for nano-spheres). Thus, the convective loss rate $\frac{k}{r}(4\pi r^2)(T - T_\infty)$ (where, T_∞ is the ambient temperature) is proportional to r, while the total heat released due to chemical reaction is proportional to r^3. As a result, convective heat loss becomes significant for small spheres. An estimate shows that for an aluminum particle of radius 25 nm, all the heat released by oxidation may be lost to steady convection in a time scale of 10^{-8} s, which is comparable to the time scale of the final rapid phase of the oxidation process in our model. Radiation loss $4\pi\sigma_b r^2 T^4$, where σ_b is the Stefan–Boltzmann constant, contributes less than convection for the values of parameters in our model (radiation loss exceeds the convection at high temperatures $T \gg \left(\frac{k}{\sigma_b r}\right)^{\frac{1}{3}}$, which is of order $10^4\,\mathrm{K}$ for $r = 25\,\mathrm{nm}$).

We note that Eq. (3) for the metal boundary velocity is similar to the model of metal sphere oxidation considered in Ref. 1; however, self heating was not included. Mohan *et al.*[4] describe initial stages of Cabrera-Mott mechanism and predict Al oxidation on a 100 ns time scale using the Coulomb potential for a particle of radius 10 nm with a very thin initial oxide layer. The principal mechanism considered in Ref. 4 is very fast temperature rise, the temperature increases from 650 to over 2200 K, while oxide thickness increases from 0.3 to 0.5 nm. We use the self-consistent potential (a solution of the nonlinear Poisson equation (1)

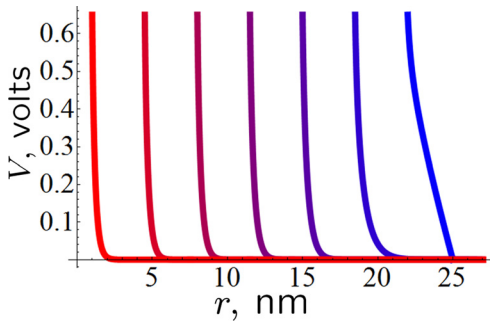

FIG. 1. Self-consistent potential V for $r_1 = 2, 6, 10, 14, 18, 22$ nm. Here, $r_{10} = 22$ nm, $r_{20} = 25$ nm, $V_0 = 0.65$ V, $\phi + W_i = 1.5$ V, $W = 1.7$ V, $T_0 = 750$ K.

rather than the Coulomb potential) and experimental measured maximum temperature to model the self-heating. As a result, oxidation rates are dramatically increased, while the maximal temperature is still not too high and is matched with the experimental data.[12]

We have found the self-consistent potential V, solving numerically the boundary value problem for the Poisson equation (1) for various radii r_1 (we have used the Newton's method to solve a discrete version of the problem). Our results for the potential are illustrated in Figure 1. Our values of ionization parameters $V_0 = 0.65$ V, $\phi + W_i = 1.5$ V, $W = 1.7$ V, $a = 0.4$ nm are consistent with the data in the Cabrera-Mott paper.[7] We used $r_{10} = 22$ nm for the initial metal radius, and $r_{20} = 25$ nm for the initial metal + oxide radius. When the remaining metal radius is $r_1 \le r_{10}$, the radius of the metal + oxide r_2 can be found from Eq. (4), and the temperature, with the self heating taken into account, is determined by Eq. (5). We use $T_0 = 750$ K as the initial temperature.

Solution of the nonlinear Poisson equation (1) enables us to compute the gradient of the potential on the metal surface, and corresponding potential decrease due to electric field near metal-oxide interface, for various radii r_1. In Figure 2, we show electric potential decrease at a distance $a = 0.4$ nm from the metal-oxide interface for the solution of nonlinear Poisson equation (solid line), and compare it with a potential decrease computed using Coulomb potential (broken line). Potential decrease determines oxidation speed, via an exponential Gibbs factor in Eq. (3). Our results demonstrate that the nonlinear model for the potential, with the self-heating effect, yields considerably higher oxidation rates.

Using results for the gradient of the potential on metal-oxide boundary, we can find the radius of the metal sphere as a function of time, by solving the moving boundary Eq. (3). This equation is separable, since it follows from Eqs. (4) and (5) that the right hand side is a function of r_1 only. Thus, a solution can be found by a numerical integration. The solution is shown in Figure 3. The overall oxidation time scale is in microseconds, much faster than for macroscopic particles. We further observe that in our model most of oxidation occurs very quickly towards the end of oxidation process, since reaction rate dramatically increases with the temperature rise due to the self-heating.

Our model yields oxidation time of 32 μs for a spherical aluminum nanoparticle of radius 25 nm at initial temperature of 750 K. Using exactly the same ionization parameters and the self-heating mechanism, but taking the Coulomb potential rather than a solution of the self-consistent equation (1), oxidation time is calculated to be 2.5 ms, that is, almost 100 times slower. We note that the diffusion limit corresponds to the linear in the Coulomb potential V' approximation of the Eq. (3). It is clear from Eq. (3) that the oxidation rate in the linearized model will be much slower than for the Mott model. Using the same model parameters and the self heating as in our model, oxidation time in the diffusion limit would be about 40 ms; and without the self-heating it is estimated to be 14 s at $T = 750$ K. Experimentally, an explosive oxidation reaction of nanosized particles is initiated at a temperature of about 750 K (i.e., below aluminum melting temperature), with the reaction time scale estimated to be in microseconds.[12] This comparison strongly suggests the Cabrera-Mott model with a self-consistent potential as the most likely reaction mechanism.

Figure 4 illustrates the oxidation rate of change of mass of aluminum in a metal-oxide sphere with initial radius 25 nm, as a function of aluminum mass and temperature T. Such a rate of change of reacting mass appears, e.g., in Semenov explosion model, with $\frac{1}{m}\frac{dm}{dt}$ usually given by the Arrhenius factor $\exp(-\frac{E}{T})$ with a constant E. However, in Cabrera-Mott oxidation model, E depends on the remaining mass and temperature (since electric potential drop in the self-consistent Cabrera-Mott model depends on the metal radius and temperature).

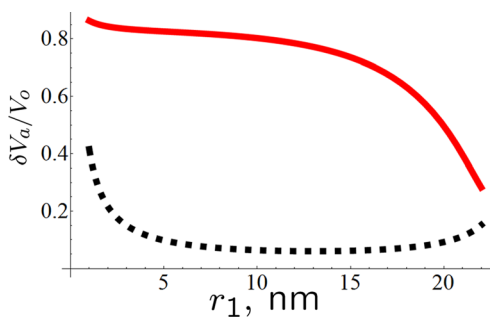

FIG. 2. Potential drop a distance $a = 0.4$ nm from aluminum metal-oxide interface, as a function of the remaining metal radius, self-heating included. Solid curve: nonlinear self-consistent potential; dashed curve: Coulomb potential. Here, $V_0 = 0.65$ V, $r_{10} = 22$ nm, $r_{20} = 25$ nm, $\phi + W_i = 1.5$ V, W = 1.7 V, $T_0 = 750$ K, $T_M = 2273$ K.

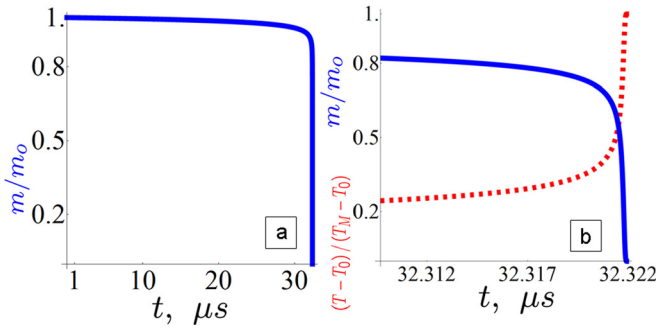

FIG. 3. Oxidation time scales: (a) ratio of remaining aluminum metal mass to initial aluminum mass, as a function of time. Here, $r_{10} = 22$ nm, $r_{20} = 25$ nm, $\phi + W_i = 1.5$ V, $W = 1.7$ V, $T_0 = 750$ K, $T_M = 2273$ K, $a = 0.4$ nm. (b) Final stages of oxidation shown; solid curve: remaining metal mass, dashed curve: temperature.

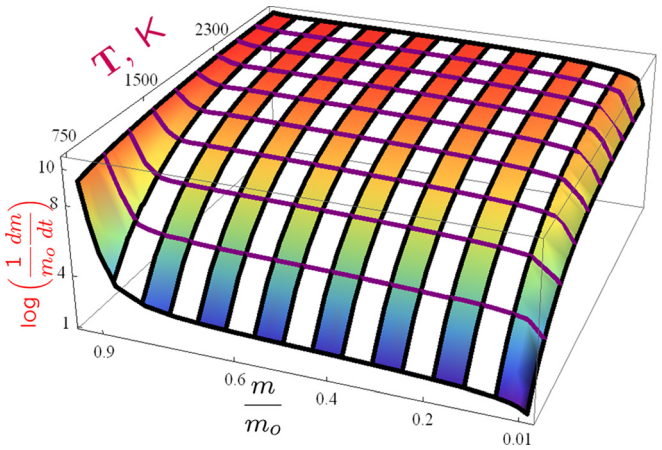

FIG. 4. Oxidation rate of change of mass of metal aluminum in a metal-oxide sphere of initial radius 25 nm, as a function of metal mass m and temperature T (K), in $\log_{10}$ scale. Metal mass is shown as a ration to the initial mass of the particle m_0. Here, initial radius is 25 nm, $\phi + W_i = 1.5$ V, $W = 1.7$ V, $T_0 = 750$ K, $T_M = 2273$ K, $a = 0.4$ nm.

Nonlinearity in equation for the self-consistent electric potential, together with the self-heating effect, leads to significant increase of oxidation rate for nano-sized aluminum particles, compared to the model with Coulomb potential and without self-heating. Results of our modeling suggest oxidation time scales in microseconds range for nano-sized aluminum particles, in agreement with the experimental evidence.[12] Results of computation of oxidation time scale are very sensitive to values of ionization potentials, since they appear as Gibbs factors in the equation for boundary velocity. Therefore, we expect that oxidation rate will be very sensitive to defects, and to deviation from spherical symmetry.

We acknowledge the financial support of this research by the National Science Foundation Grants 0933140 and HRD-1242090.

[1]A. Ermoline and E. L. Dreizin, Chem. Phys. Lett. **505**, 47 (2011).
[2]V. P. Zhdanov and B. Kasemo, Chem. Phys. Lett. **452**, 285 (2008).
[3]V. P. Zhdanov and B. Kasemo, Appl. Phys. Lett. **100**, 243105 (2012).
[4]S. Mohan, A. Ermoline, and E. L. Dreizin, J. Nanopart. Res. **14**, 723 (2012).
[5]S. K. R. S. Sankaranarayanan, E. Kaxiras, and S. Ramanathan, Phys. Rev. Lett. **102**, 095504 (2009).
[6]N. W. Piekiel, K. T. Sullivan, S. Chowdhury, and M. R. Zachariah, "The role of metal oxides in nanothermite reactions: Evidence of condensed phase initiation," U.S. Army Research Office Technical Report No. 55832-EG.2, 2010.
[7]N. Cabrera and N. F. Mott, Rep. Prog. Phys. **12**, 163 (1949).
[8]A. T. Fromhold and E. L. Cook, Phys. Rev. **158**, 600 (1967); **163**, 650 (1967).
[9]A. T. Fromhold, *Theory of Metal Oxidation* (North Holland, 1975).
[10]D. D. Dlott, Mater. Sci. Technol. **22**, 463 (2006).
[11]E. L. Dreizin, Prog. Energy Combust. Sci. **35**, 141 (2009).
[12]K. S. Martirosyan, J. Mater. Chem. **21**, 9400 (2011).
[13]S. F. Son, B. W. Asay, T. J. Foley, R. A. Yetter, M. H. Wu, and G. A. Risha, J. Propul. Power. **23**, 715 (2007).
[14]K. Sullivan, G. Young, and M. R. Zachariah, Combust. Flame **156**, 302 (2009).
[15]J. A. Puszynski, C. J. Bulian, and J. J. Swiatkiewicz, J. Propul. Power **23**, 698 (2007).
[16]K. Moore and M. L. Pantoya, Propellants, Explos., Pyrotech. **31**, 182 (2006).
[17]K. S. Martirosyan, L. Wang, A. Vicent, and D. Luss, Nanotechnology **20**, 405609 (2009).
[18]K. S. Martirosyan, L. Wang, A. Vicent, and D. Luss, Propellants, Explos., Pyrotech. **34**, 532 (2009).
[19]K. S. Martirosyan, L. Wang, and D. Luss, Chem. Phys. Lett. **483**, 107 (2009).
[20]K. S. Martirosyan, M. Zyskin, C. M. Jenkins, and Y. Horie, J. Appl. Phys. **112**, 094319 (2012).
[21]R. Byron Bird, W. E. Stewart, and E. N. Lightfoot, *Transport Phenomena*, 2nd ed. (John Wiley & Sons, 2006).